Comparison of Bifacial Solar Irradiance Model Predictions With Field Validation

Silvana Ayala Pelaez, Chris Deline, Sara M. MacAlpine, Bill Marion, Joshua S. Stein, and Raymond K. Kostuk

***Abstract*—Models predicting rear irradiance for bifacial systems are critical to establish accurate estimates of energy yield. Here, we compare five published bifacial irradiance models, varying clearance, row spacing, tilt, and albedo to measure the sensitivity to these parameters. Bifacial energy gains (BG_E) as high as 20% are predicted for some configurations. Model agreement is generally good for low ground clearance (clearance heights lower than 0.75 times the collector width), but at higher clearances, finite system size and edge effects become a significant factor in simulations, stretching assumptions of infinite system extent made in some models. In addition, rear irradiance uniformity is improved at high ground clearance, as expected. A test-bed construction and results are described for comparison between modeled and measured data in Golden, CO, USA. The investigations indicate that model agreement for BG_E calculation is better than 2% (absolute) when compared with measured results, depending on the system configuration.**

***Index Terms*—Bifacial solar panels, irradiance modeling, photovoltaic (PV) system modeling.**

I. Introduction

BIFACIAL solar panel technology has been around since 1977 [1], but has gained renewed attention due to recent cost reductions, with bifacial market share projections reaching 30% by 2027 [2]. Monofacial panels collect only front-side incident light, but bifacial panels can take advantage of both sides to increase their collection area. Energy yield can increase significantly with the collection of rear diffuse and ground-reflected energy, which depends greatly on climate and system configuration [3]–[5]. This is a strong motivation for the use of bifacial modules, but uncertainty exists around expected performance for individual system configurations.

Back surface irradiance is a result of illumination and system parameters. Illumination is dependent on the geographical location's conditions due to sun position, direct and diffuse radiation components, and climate. System parameters to consider are row-to-row distance, clearance from the ground, tilt, and the albedo of the underlying surface. Techniques for back surface irradiance modeling fall into three categories: ray-tracing models, which simulate multipath reflection and absorption of individual rays entering a scene [6]–[8]; view factor approaches, which assume isotropic scattering of reflected rays and so permit calculation of irradiance by integration [9]–[11]; and empirical models representing the relationship between measured quantities, e.g., between direct and diffuse irradiance, and measured back surface irradiance [12]. A comparison of three bifacial models has been published previously [13], where measurement and simulations for front and rear irradiance for one sample day showed good consistency at cell and module levels. Several previous publications have investigated the performance of one bifacial module in isolation [13]–[15]. In this paper, we look at the effects of multiple rows and multiple modules in a row and their effect on module performance. Adjacent modules generate mutual shading for modules within the row and adjacent rows. A scaled test bed is presented for comparing the performance predicted by the different models to measured data.

II. Metrics

Bifacial modules are characterized by their bifaciality factor φ_{Pmp}, which is defined by the ratio of rear and front 1-sun power [16]

$$\varphi_{\mathrm{Pmp}} = \frac{\mathrm{Pmp,\ rear}}{\mathrm{Pmp,\ front}} \times 100\%. \tag{1}$$

Bifaciality factors vary with cell and module design, with values reported in the literature as high as 99% [17], but usually ranging commercially between 60% and 90% [14], [18]. The potential energy gains of using a bifacial panel instead of a monofacial panel can be estimated from the front and

Manuscript received June 18, 2018; revised August 22, 2018 and October 4, 2018; accepted October 10, 2018. Date of publication November 14, 2018; date of current version December 21, 2018. This work was authored in part by Alliance for Sustainable Energy, LLC, the manager and operator of the National Renewable Energy Laboratory for the U.S. Department of Energy. This work was supported in part by the U.S. Department of Energy under Contract DE-AC36-08GO28308 with the National Renewable Energy Laboratory, in part by the U.S. Department of Energy under Grant BS123456, and in part by the Engineering Research Center Program of the National Science Foundation (NSF) and the Office of Energy Efficiency and Renewable Energy of the Department of Energy under NSF Cooperative Agreement EEC-1041895. This work was also supported by the U.S. Department of Energy's Office of Energy Efficiency and Renewable Energy under Solar Energy Technologies Office Agreement 30295. Any opinions, findings, and conclusions or recommendations expressed in this material are those of the author(s) and do not necessarily reflect those of the NSF, the Department of Energy, or the U.S. Government. *(Corresponding author: Silvana Ayala Pelaez.)*

S. Ayala Pelaez and R. K. Kostuk are with the University of Arizona, Tucson, AZ 85719 USA (e-mail: silvanaa@email.arizona.edu; kostuk@email.arizona.edu).

C. Deline and B. Marion are with the National Renewable Energy Laboratory, Golden, CO 80401 USA (e-mail: chris.deline@nrel.gov; bill.marion@nrel.gov).

S. M. MacAlpine was with the National Renewable Energy Laboratory, Golden, CO 80401 USA. She is now with juwi Inc, Boulder, CO 80301 USA (e-mail: smacalpine@juwiamericas.com).

J. S. Stein is with Sandia National Laboratories, Albuquerque, NM 87185 USA (e-mail: jsstein@sandia.gov).

Color versions of one or more of the figures in this paper are available online at http://ieeexplore.ieee.org.

Digital Object Identifier 10.1109/JPHOTOV.2018.2877000

rear irradiance

$$BG_E\,[\%] = \varphi_{\mathrm{Pmp}} \times \frac{G_{\mathrm{rear}}}{G_{\mathrm{front}}}\,(1 - \eta_{\mathrm{loss}}) \tag{2}$$

where G_{front} and G_{rear} are the front and rear average incident irradiances, respectively. The η_{loss} term reflects that power and energy production can be affected by mismatch effects, resulting from the nonuniform rear-side irradiance and rear shading. Reference cells matched for spectrum and incidence angle can be used to measure the front and rear irradiances. To evaluate uniformity, more than one sensor is needed for each side and is calculated with the maximum and minimum rear-side irradiances

$$\text{nonuniformity} = \frac{\max G_{\mathrm{rear}} - \min G_{\mathrm{rear}}}{\frac{1}{2}\,(\max G_{\mathrm{rear}} + \min G_{\mathrm{rear}})}. \tag{3}$$

For the comparisons, presented in this paper, $\varphi_{\mathrm{Pmp}} = 100\%$ and $\eta_{\mathrm{loss}} = 0\%$ have been assumed for simplicity.

The main geometric factors to consider for bifacial systems include the row-to-row pitch R and the ground clearance height H in meters, measured from the ground to the bottom edge of the module. Normalized values are expressed in terms of a ground coverage ratio gcr = CW/R, where CW is the photovoltaic (PV) collector width (overall width of the modules in a row). Similarly, normalized clearance height $h = H/$CW.

A. Existing Bifacial Performance Models

Bifacial system performance models utilize different methods to calculate the rear irradiance contribution and fall into three general categories [13]: raytracing models, view factor models, and empirical models. An overview of five publicly available models considered in this work can be seen in Table I.

Ray-tracing models offer the possibility of reproducing complex scenes but are often more computationally intensive. For yearly simulations, techniques like pre-processing of a cumulative sky for the year can reduce simulation time by over 1000× [19]. The National Renewable Energy Laboratory (NREL) has developed a bifacial-specific application leveraging the Radiance [20] ray-tracing software to generate scene geometries for evaluating bifacial system performance over the course of a year from measured or typical meteorological irradiance data. In this open-source software toolkit (called bifacial_radiance [21]), irradiance can be calculated for any location in the array, making it an ideal tool to study edge effects resulting from the array's size. The ray-tracing engine also allows custom specification of nearby shade obstructions including self-shading from PV array rack structures.

View factor or configuration factor models calculate the fraction of irradiance scattered or reflected from surfaces adjacent to a collection location on a bifacial PV cell module. In this paper, two bifacial view factor models are considered: one developed at the NREL [9] and the other is part of the commercial PVSyst software [22]. Both methods simplify bifacial system geometry to consider regular row layouts of infinite extent, resulting in fast runtime and low computer memory requirements.

Diffuse-sky and direct-beam solar irradiance are calculated for the rear of the module based on the incidence angle and sky view factor. Ground-reflected irradiance (GRI) is calculated in a two-part process. First, ground-incident irradiance between rows is calculated in n segments, where each ground segment is identified as either shaded or unshaded by adjacent rows. The incident ground irradiance for the nth segment GRI_n is calculated by

$$\mathrm{GRI}_n = a \cdot \mathrm{DNI} + \mathrm{CF}_{\mathrm{sky}} \cdot I_{\mathrm{sky}} \tag{4}$$

where a is the cosine of the sun zenith angle if the ground segment n is unshaded. $\mathrm{CF}_{\mathrm{sky}}$ is the view factor of the open sky by ground segment n, and I_{sky} is the isotropic sky diffuse irradiance.

The GRI received by the m segments of the back side of the PV module is then calculated by summing the contribution to each of the m panel segments from each of the n ground segments, multiplied by the ground albedo and view factor to the rear of the module.

Overall bifacial system power production can be evaluated by multiplying front-side effective irradiance by $(1 + BG_{\mathrm{E}})$ from (2). This total effective irradiance can include back-side mismatch loss (η_{loss}) and rear shading loss to account for shading caused by the mounting structure, cabling, and junction boxes. Calculating these values is beyond the scope of this current work, and η_{loss} is assumed = 0% here.

TABLE I
REAR IRRADIANCE MODEL COMPARISON

Quantity	Prism Solar	Solar World	PV Syst	NREL VF	Radiance
Albedo, tilt, *h*, *gcr*	✓[1]	✓	✓	✓	✓
Panel size	X[2]	✓[3]	✓	✓[3]	✓
BG_E calculated	By year	By year	By hour	By hour	By year
Running time for yearly simulation[4]	<1s	<1s	<10s	<10s	<60s
Irradiance profiles	-	-	?	✓	✓
Ground incident irradiance model	-	-	✓[5]	✓[6]	✓[6]
Glass-air transmission loss	-	-	?	✓[7]	-
Light transmitted between cells	-	-	✓	✓	opt.
Shading losses	-	-	✓[8]	-	✓
Specific number & size of rows	-	-	Infinite	Infinite	✓
Edge effects modeled	-	-	-	-	✓
1-axis tracking	-	-	✓[9]	✓	✓

[1]Row spacing is assumed to be equal to or larger than the typical row spacing at noon on December 21st.
[2]Considers panel size Bi48/B200 and B245/B250/B260/Bi60/Bi72.
[3]Geometry is scaled relative to the collector width.
[4]The simulations were performed on a Dell Inspiron 7737 computer equipped with an Intel Core i7-4510U processor and 8 GB of RAM running a 64-bit version of Windows 8.1. Seven rows of 20 modules were assumed for the raytrace.
[5]Isotropic diffuse sky irradiance.
[6]Perez diffuse sky irradiance
[7]Glass–air transmission loss for rear-side beam and diffuse irradiance.
[8]PVsyst considers mechanical structures behind the module, like from the mounting structures, cabling, and the junction box, with a shading factor.
[9]Starting with v6.70 PVSyst includes one-axis tracking bifacial support.

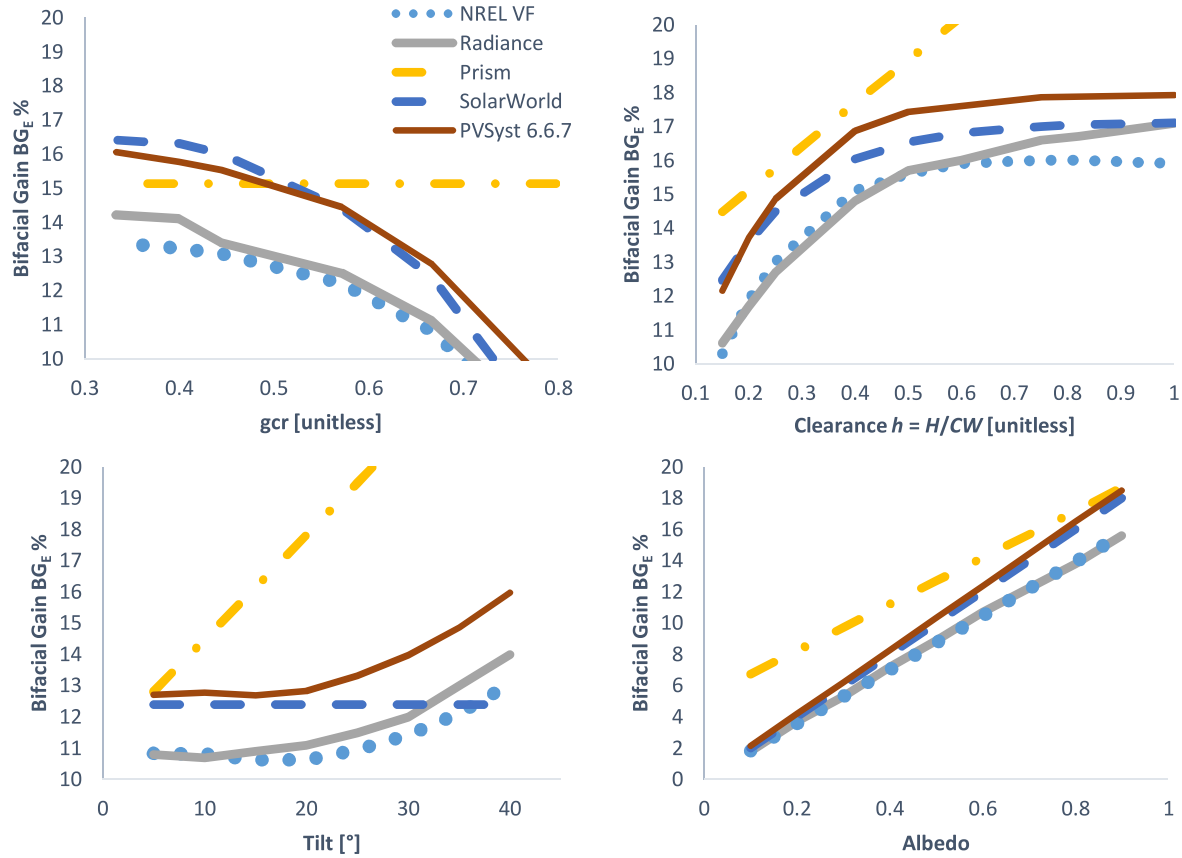

Fig. 1. Yearly back-side irradiance gain ratio comparison for different bifacial PV rear-side irradiance models, varying module tilt, module height, row-to-row pitch, and ground albedo, for Richmond VA location. Default values (when not varied) are gcr = 0.66, clearance $h = 0.15$, albedo = 0.62, tilt = 10°, and collector width = 1 m. BG_E is equal to G_{rear}/G_{front} for $\varphi_{Pmp} = 100\%$ and $\eta_{loss} = 0\%$.

Although only fixed-tilt systems are considered in this paper, both NREL's VF and Radiance models allow single-axis tracking configurations to be considered.

The empirical models are simplified analytical approximations based on a combination of measurements and simulation, which use a more limited set of variables to calculate an approximate bifacial gain per year. One model based on system-level ray-tracing simulations was proposed by Kutzer *et al.* [23] and made available by manufacturer SolarWorld through a web interface [24]. Input variables are albedo, normalized clearance height $h = H/\text{CW}$, and ground coverage ratio gcr. BG_E is then calculated as follows:

$$BG_E\,[\%] = \text{Albedo} * \varphi_{Pmp} * 0.95\,[1.037\,(1 - \sqrt{\text{gcr}}\,)\,(1 - e^{-8.691 * h * \text{gcr}}) + 0.125\,(1 - \text{gcr}^4)] \quad (5)$$

where $BG_E[\%]$ is the additional bifacial energy gain in percent, relative to a monofacial module [as in (2)]. Note that this model does not include the effects of tilt, orientation, or climate.

A second empirical model developed by Castillo-Aguilella and Hauser from Prism Solar Technologies also allows yearly bifacial gain calculation for single modules [12]. Although climate is not specifically considered, the model is suggested for latitudes between 21° and 51° from the equator, and ground shading from adjacent rows is not considered. BG_E is assumed to increase with the tilt angle, with values between 7.5° and 35°. Row-to-row spacing is assumed to be enough for the module installation in landscape or portrait to avoid self-shading. Only equator-facing modules are considered, and no racking or structural shading are accounted for. Their equation for BG_E is

$$BG_E\,[\%] = a \cdot \text{tilt} + b \cdot H + c \cdot \text{Albedo}\,[\%] \quad (6)$$

where a is the curve-fitting coefficient for the tilt angle in degrees, b for the clearance height of the module in meters, and c for the albedo in percent. The values for these coefficients were found by incorporating NY and AZ test data and are $a = 0.317/°$, $b = 12.145/\text{m}$, and $c = 0.1414/\%$. Given that Prism Solar assumes panels of bifaciality ratio $\varphi_{Pmp} = 95\%$, in order to compare between the models in this paper, the result of BG_E [see (6)] was divided by 0.95.

B. Comparison of Performance Models

We conducted a comparison of annual BG_E for the models listed in Table I as a function of the tilt angle, albedo, gcr, and clearance height (see Fig. 1). To maintain consistency between models, the input geometry is expressed in terms of the PV system collector width CW = 1 m for a 1-up landscape configuration. The base parameters assume a close-mount rooftop system with the gcr of 0.66, the ground clearance of 0.15 m, albedo of 0.62, and a tilt of 10°. For the model

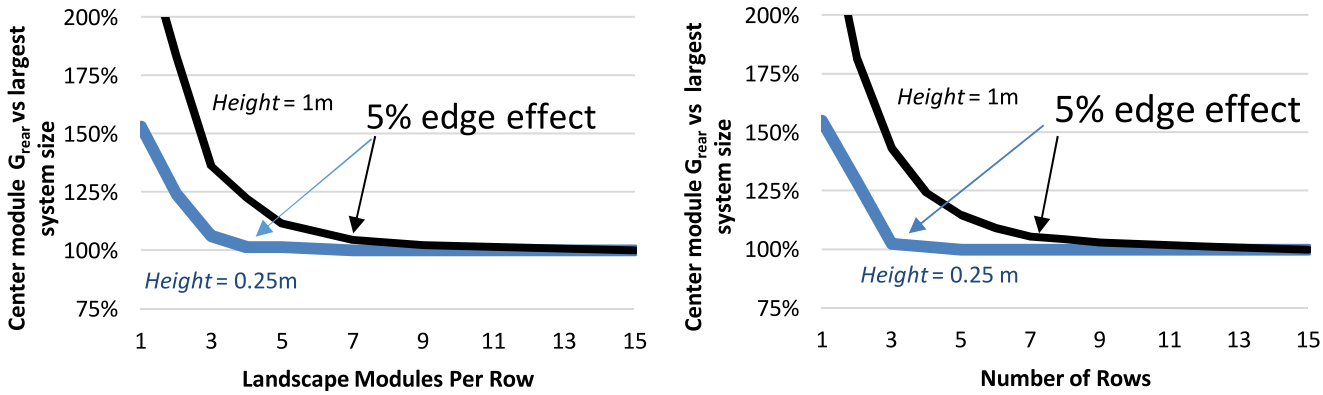

Fig. 2. BG_E for small systems is compared with a semi-infinite (20 module, seven rows) assumption. Edge effects for different heights H and system sizes are evaluated through ray tracing, using the same configuration assumed in Fig. 1. Collector width CW equals 1 m for the simulation.

comparisons, the same TMY3 climate file is used for Richmond, VA, USA.

As can be seen in Fig. 1, the predicted annual rear-side irradiance gain follows similar trends for the more complicated models. The two empirical models are less accurate at following the more detailed trends. In particular, the Prism empirical model is less accurate at higher gcr, height, and tilt angle. The remaining models compare well, within an absolute BG_E range of 2%–3%. Of the three nonempirical models, the NREL VF model is the most conservative, maintaining an absolute 2% lower performance prediction relative to the PVSyst 6.6.7 model. The Radiance and SolarWorld empirical models fall in between these two values.

C. System Size and Edge Effect Sensitivity

The effect of the finite size of the array can be of significance if the system is not large enough to cast representative shade conditions [25]. Since the view factor models considered here have an implicit assumption of infinite row extent, ray-tracing models are required to evaluate the true impact of smaller system installations, or "edge effects" (EE), defined as

$$\mathrm{EE} = \frac{\mathrm{BG_E}\,(\#\mathrm{rows}, \#\mathrm{modulesperrow})}{\mathrm{BG_E}\,(\infty\mathrm{rows},\ \infty\mathrm{modulesperrow})}. \tag{7}$$

Fig. 2 investigates how many modules per row are required to meet the semi-infinite assumption at the center of the array, as well as the number of rows in the system that are required. The geometry assumptions from Fig. 1 are used again here (1.5-m row spacing, albedo of 0.62, and a tilt of 10°) and $h = 0.25$ or 1. The Radiance results show that the system size required to approximate an infinite extent requires a larger field size at higher array height h. Specifically, for a low $h = 0.25$, an array with three rows and four modules per row is large enough to achieve G_{rear} within 5% of a semi-infinite assumption at the center module. At $h = 1$, a larger array of seven rows with seven modules per row (~15 kW) would be required to meet this same criterion. Note that the modules at the edges of large bifacial arrays will still experience higher G_{rear} than the center module considered here. These optical models, therefore, represent a conservative approximation of irradiance.

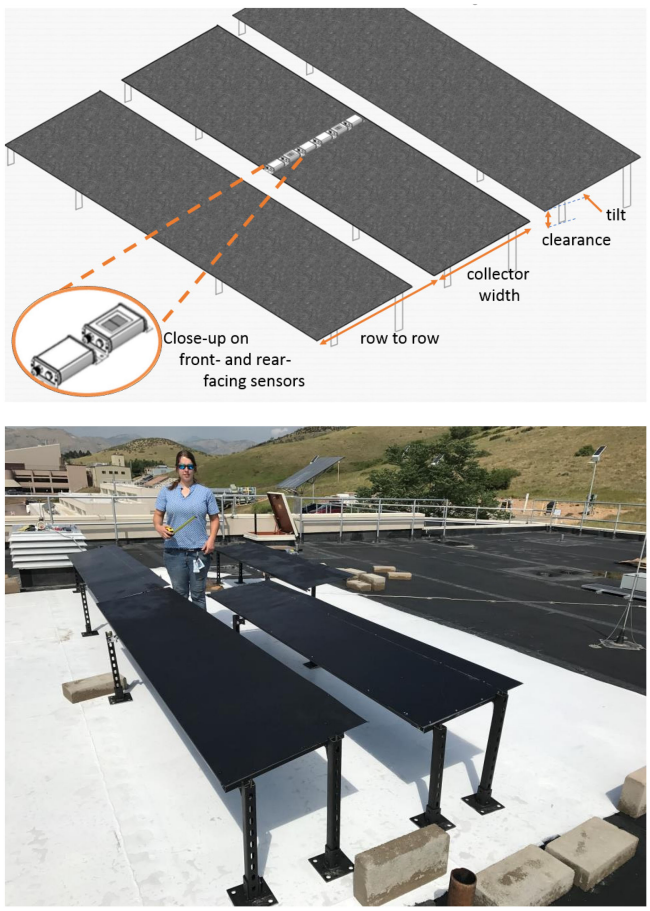

Fig. 3. Diagram (top) of the field test bed built in Golden, CO, USA, with two front-facing and four back-facing irradiance sensors. The array can be modified for row-to-row spacing, tilt angle, and clearance height. Photograph (bottom) shows array under construction, ballasts, and the white roof coating.

III. Field Validation Test Bed

A mock array approximating the above high albedo roof-mount conditions was constructed from three rows of 20-ft by 2-ft aluminum "panels," which are supported with a strut channel structure (shown in Fig. 3). The modular design allows modifications of height, row spacing, and panel tilt. The panels'

TABLE II
TEST-BED CONFIGURATIONS, RELATIVE TO THE COLLECTOR WIDTH

Setup	Tilt	Row to Row	Clearance	Albedo	Dates
1	10	1.5	0.82	0.7	8/11-8/24
2	10	1.5	0.6	0.7	8/25-9/1
3	10	1.5	0.15	0.7	9/2-9/11
4	10	2	0.15	0.62	9/12-10/2
5	10	3	0.15	0.62	10/3-10/8
6	10	3	0.4	0.56	10/18-10/30
7	10	2	0.4	0.56	10/30-11/13
8	10	1.5	0.4	0.56	11/14-12/8

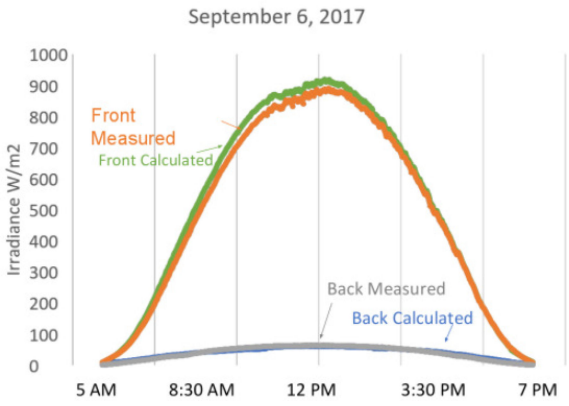

Fig. 4. Average irradiance value measured with the front and back sensors, versus modeled (view factor) irradiances. Agreement for front sensors is <1% RMS, and back sensors is <2.3% RMS through the day.

azimuth was set to 180° (equator facing). The ground and the ballast were painted with a 100% silicone white roof coating. The reflectivity of the surface was measured at the beginning and end of the experiment and decreased from 0.74 to 0.56, as discussed in more detail in the following.

Fig. 3 shows the location for two forward-facing and four rear-facing irradiance sensors (IMT Si reference cells) deployed in the middle of the array, across the middle module's slope. The field of view from the downward-facing sensors is judged to be un-impaired by vertical mounting struts out to a lateral distance of 1.2 m, or a zenith angle of 60–70°. All mounting strut and shading panels were painted black to reduce reflections from adjacent rows.

Data were gathered over a period of three months, from August to November 2017, for the different configurations shown in Table II. The variable height and row spacing are shown relative to the landscape width of the modules. Direct normal irradiance and diffuse horizontal irradiance measurements from the nearby Solar Radiation Research Laboratory Baseline Measurement System [26] were used as inputs to NREL's view factor and Radiance models to calculate the irradiance profiles at the sensor' locations at 5-min intervals. Fig. 4 shows an example for average measured and average modeled data with the view factor model for a day in setup 3 (normalized height H/CW = 0.15, row spacing R/CW of 1.5, and tilt of 10°). The measurements from the sensors and the calculated rear irradiance had less than 2.3% RMS error for the day shown.

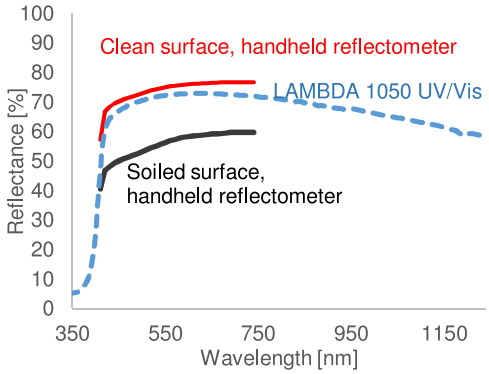

Fig. 5. Reflectance of roof coating used for test bed, measured in spectrophotometer, and *in situ* with a handheld spectrophotometer for clean and soiled surfaces at the end of the experiment.

A. Albedo and Soiling

The reflectivity of the roof surface was measured at the beginning of the experiment using a benchtop Lambda 1050 spectrophotometer and was also measured at the beginning and end of the experiment with a Konika CM700D handheld spectrophotometer. Initial measurement by the two instruments showed 0.7 reflectance for a clean surface. By the end of the four-month experiment, soiling had reduced surface reflectance to 0.56 (see Fig. 5).

Because albedo measurements were not taken continuously during the experiment, assumptions of surface albedo must be made for each model comparison. As shown in Table II, we are assuming consistent albedo values for each month of measurements and are, therefore, considering a value of 0.7 albedo for the first three setups, 0.62 for setups 4 and 5 during which most of the liquid precipitation was received for the experiment, and 0.56 for the last three setups. Uncertainties arising from these albedo assumptions are considered in error bars in the following.

B. Field Validation Results

Average BG_E values measured for the eight deployment conditions of Table II are shown in Fig. 6. In general, these cumulative average results show good agreement between the experiment and the Radiance and view factor models. In particular, the view factor model has better agreement for lower clearances of $h < 0.6$, and for higher clearances, it under-predicts. This difference is due in part to the Radiance model's ability to account for the system's smaller-than-optimal row count = 3. As discussed above, edge effects become more pronounced for small systems as system clearance heights are increased.

Error bars of 1%–2% are also shown here accounting for soiling and surface albedo effects mentioned above, in addition to spatial positioning uncertainty and irradiance sensor accuracy. The effect of nonuniform illumination on mismatch loss and BG_E has not been considered here, but spatial distribution of rear irradiance was recorded and is shown in the following.

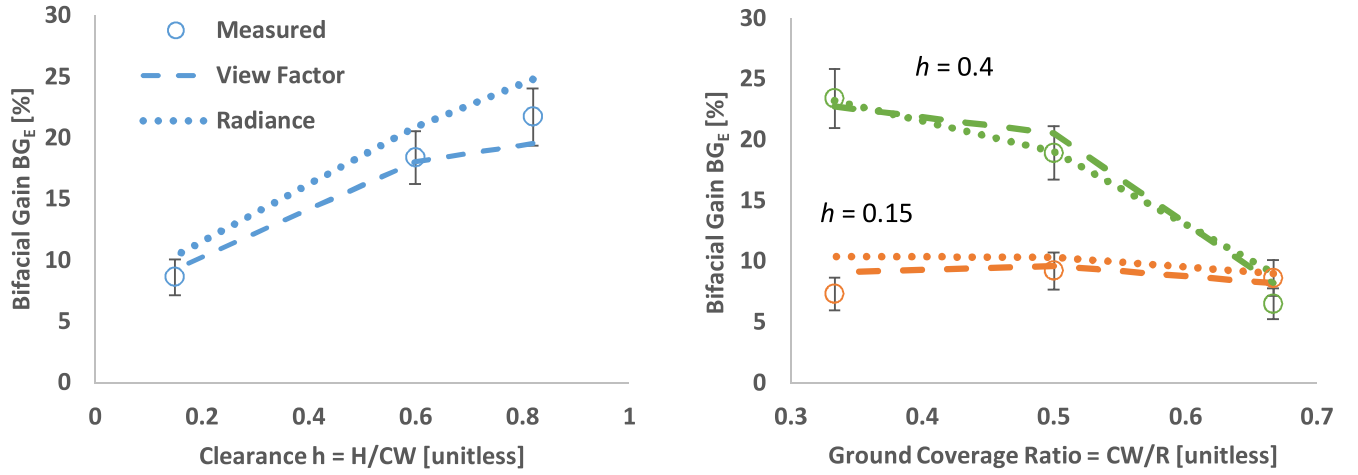

Fig 6. Measured and modeled results for the test bed. Clearance height h and row spacing r are normalized by the mock array collector width of CW = 0.61 m. Measurement uncertainty is driven by soiling of the roof surface and reference cell uncertainty at low irradiance.

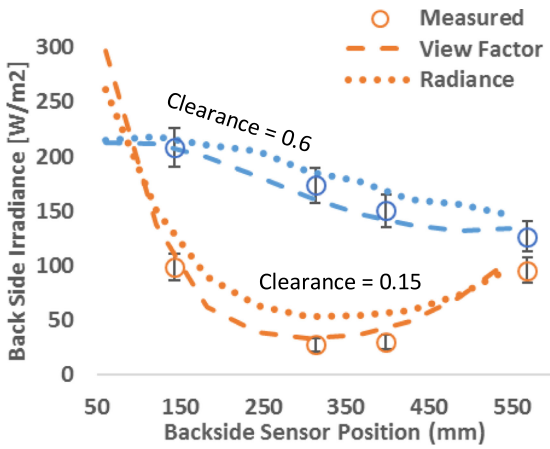

Fig. 7. Rear irradiance distribution for 9/1 ($h = 0.6$) and 9/2 ($h = 0.15$) at noon. At $h = 0.15$, the light reaching the middle sensors is lower than the bottom and top sensors, and spatial nonuniformity is high.

Fig. 7 shows the measured and modeled rear irradiance for two consecutive days with different h, taken at the same time of day. The spatial nonuniformity across the field-measured points is 23% for $h = 0.15$, with the average being 82 W/m^2. If you include all simulated points, the nonuniformity goes up to 40%. For $h = 0.6$, the nonuniformity is 16% for measured points at an average of 169 W/m^2. This shows good agreement between the models and this measurement within experimental uncertainty. We can, therefore, confirm good model agreement both at fine spatial/temporal resolution, as well as averaged over longer-term conditions and over the array width.

IV. Conclusion

A comparison among five models has been presented for determining bifacial power boost. The models vary in complexity with the Radiance model being the most complex and comprehensive. Commercial models like PVSyst and NREL's view factor model are based on the semi-2D assumption, and models like Solar World and Prism Solar are based on empirical fits to particular setups. Despite their differences in assumptions and complexity, there is a good agreement between all models, particularly for low ground clearance conditions. At higher ground clearance, the influence of edge effects become more pronounced and may not be accurately modeled by all methods. A test bed has been built to validate the results of NREL's view factor and Radiance models under different configurations. The Radiance model has been used to evaluate edge effects at different heights, noting that they become more prevalent at higher clearances. Soiling effects have been documented for the testbed, representing a 25% reduction of the albedo. Field test-measurements show good agreement within 2% error (absolute) in BG_E for the majority of conditions considered here. Nonuniformity of rear-side irradiance has also been documented using various reference cells and found to be more significant at lower clearances. Several of the other commercial and empirical simulation methods that were also considered here produced comparable bifacial gain results within model and measurement uncertainty.

References

[1] A. Cuevas, "The early history of bifacial solar cells," in *Proc. 20th Eur. Photovolt. Sol. Energy Conf.*, 2005, pp. 801–805.
[2] SEMI P V, "Group 2017 international technology roadmap for photovoltaic (ITRPV. net), Results 2016 (8th Edition)," 2016.
[3] Y. K. Chieng and M. A. Green, "Computer simulation of enhanced output from bifacial photovoltaic modules," *Prog. Photovolt.*, vol. 1, no. 4, pp. 293–299, 1993.
[4] L. Kreinin *et al.*, "PV module power gain due to bifacial design. Preliminary experimental and simulation data," in *Proc. 35th IEEE Photovolt. Spec. Conf.*, 2010, pp. 2171–2175.
[5] U. A. Yusufoglu *et al.*, "Analysis of the annual performance of bifacial modules and optimization methods," *IEEE J. Photovolt.*, vol. 5, no. 1, pp. 320–328, Jan. 2015.
[6] C. W. Hansen *et al.*, "A detailed model of rear-side irradiance for bifacial PV modules," in *Proc. 44th IEEE Photovolt. Spec. Conf.*, Washington, DC, USA, 2017, pp. 1–6.
[7] C. Deline *et al.*, "Evaluation and field assessment of bifacial photovoltaic module power rating methodologies," in *Proc. 43rd IEEE Photovolt. Spec. Conf.*, Portland, OR, USA, 2016, pp. 3698–3703.
[8] C. K. Lo, Y. S. Lim, and F. A. Rahman, "New integrated simulation tool for the optimum design of bifacial solar panel with reflectors on a specific site," *Renew. Energy*, vol. 81, pp. 293–307, 2015.

[9] B. Marion *et al.*, "A practical irradiance model for bifacial PV modules: Preprint," in *Proc. 44th IEEE Photovolt. Spec. Conf.*, Washington, DC, USA, 2017, pp. 1–6.
[10] M. Chiodetti, "Bifacial PV plants: Performance model development and optimization of their configuration," M.S. thesis, KTH Roy. Inst. Technol., Stockholm, Sweden, 2015.
[11] A. Mermoud and B. Wittmer, *PVSyst User's Manual*. PVSyst SA, Satigny, Switzerland, 2014.
[12] J. E. Castillo-Aguilella and P. S. Hauser, "Multi-Variable bifacial photovoltaic module test results and Best-Fit annual bifacial energy yield model," *IEEE Access*, vol. 4, pp. 498–506, 2016.
[13] C. W. Hansen *et al.*, "Analysis of irradiance models for bifacial PV modules," in *Proc. 43rd IEEE Photovolt. Spec. Conf.*, Portland, OR, USA, 2016, pp. 138–143.
[14] J. S. Stein, L. Burnham, and M. Lave, "One year performance results for the prism solar installation at the new Mexico regional test Center: Field data from February 15, 2016 – February 14, 2017," Sandia Nat. Lab., Albuquerque, NM, USA, Sandia Rep. SAND2017-5872, 2017.
[15] *Design Guide for Bifacial Solar Modules, rev 2.1*, Prism Solar Technologies, Highland, NY, USA, 2017.
[16] V. Fakhfouri, *Photovoltaic Devices—Part 1-2: Measurement of Current-Voltage Characteristics of Bifacial Photovoltaic (PV) Devices*, IEC TS 60904-1-2 ED1, draft, 2015.
[17] H. Schulte-Huxel *et al.*, "Flip-flop cell interconnection enabled by an extremely high bifaciality of screen-printed ion implanted n -PERT Si solar cells," in *Proc. 32nd Eur. PV Sol. Energy Conf. Exhib.*, Munich, Germany, 2016, pp. 407–412.
[18] D. Buß, E. Herzog, C. Scholz, R. Zimmermann, and B. Eisenhawer, "Outdoor characterization of bifacial modules at Hanwha Q cells," presented at Bifacial Workshop 2018, Denver, CO, USA, 2018.
[19] D. Robinson and A. Stone, "Irradiation modelling made simple: The cumulative sky approach and its applications," in *Proc. Int. Conf. Passive Low Energy Archit.*, Eindhoven, The Netherlands, 2004, pp. 19–22.
[20] G. J. Ward, "The RADIANCE lighting simulation and rendering system," in *Proc. 21st Annu. Conf. Comput. Graph. Interact. Techn.*, 1994, pp. 459–472.
[21] NREL, "Bifacial_Radiance," 2018. [Online]. Available: http://github.com/NREL/bifacial_radiance
[22] A. Mermoud and B. Wittmer, "Bifacial shed simulation with PVSyst," presented at Bifacial Workshop 2017, Konstanz, Germany, 2017.
[23] M. Kutzer *et al.*, "Ertragssteigerung durch bifaciale Modultechnologie," in *Proc. 31st Symp. Photovolt. Sol. Energy*, Bad Staffelstein, Germany, 2016, pp. 1–10.
[24] SolarWorld, "Sunmodule bisun boost calculator," 2018. [Online]. Available: http://www.solarworld.de/fileadmin/calculator/?L = 1
[25] A. Lindsay, "Modelling of Single-Axis tracking gain for bifacial PV systems," in *Proc. 32nd Eur. Photovolt. Sol. Energy Conf.*, Munich, Germany, 2016, pp. 1610–1617.
[26] T. Stoffel and A. Andreas, *NREL Solar Radiation Research Laboratory (SRRL): Baseline Measurement System (BMS); Golden, Colorado (Data)*. Golden, CO, USA: Nat. Renew. Energy Lab., 1981.

Silvana Ayala Pelaez received the B.S. degree in mechatronics engineering from the Instituto Tecnológico y de Estudios Superiores de Monterrey, Monterrey, Mexico, in 2007, and the M.S. degree in optical sciences from the University of Arizona, Tucson, AZ, USA, in 2018, where she is working toward the Ph.D. degree in electrical and computer engineering.

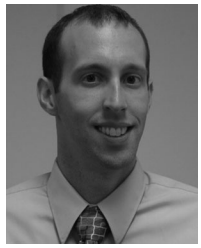

Chris Deline received the Ph.D. degree in electrical engineering from the University of Michigan, Ann Arbor, MI, USA, in 2008.

He is currently a Research Engineer with the Photovoltaic Performance and Reliability Group, National Renewable Energy Laboratory (NREL), Golden, CO, USA. He manages the U.S. Department of Energy Regional Test Center program at NREL for field assessment of novel PV technologies. He is a Principal Investigator for multiple photovoltaic field performance projects including degradation rate assessment and bifacial module power rating and production modeling.

Sara M. MacAlpine received the B.S. degree in electrical engineering from Rice University, Houston, TX, USA, in 2001, and the Ph.D. degree in civil engineering from the University of Colorado, Boulder, CO, USA, in 2014.

She spent several years investigating photovoltaic performance modeling with the National Renewable Energy Laboratory, Golden, CO. She is currently an Engineer with juwi, Inc., Boulder. Her research interests include photovoltaics and renewable energy systems.

Bill Marion received the B.S. degree in mechanical engineering from the South Dakota State University, Brookings, SD, USA, in 1978 and the M.S. degree in energy systems from the University of Central Florida, Orlando, FL, USA, in 1986.

He is currently a Principal Engineer with the National Renewable Energy Laboratory, Golden, CO, USA. He works in the area of photovoltaic (PV) module and system technology testing and evaluation, solar resource assessment, and model development. PV performance modeling activities have included PVWATTS, an internet-accessible PV simulation tool, and the development and validation of PV module *I–V* curve translation procedures.

Mr. Marion is a registered Professional Engineer.

Joshua S. Stein received the Ph.D. degree in earth sciences from the University of California, Santa Cruz, CA, USA, in 2000.

He is a distinguished member of the Technical Staff with Sandia National Laboratories, Albuquerque, NM, USA, where he leads research projects aimed at understanding and improving the performance and reliability of photovoltaic (PV) technologies. He founded the PV Performance Modeling Collaborative in 2010 and is active in the International Energy Agency's PVPS Task 13 on PV performance and reliability. His current projects are focused on bifacial PV performance and modeling and degradation rate analysis and characterization.

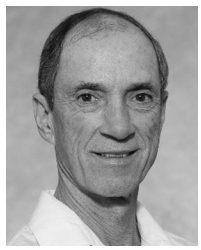

Raymond K. Kostuk received the B.S. degree in physics and mathematics from the United States Coast Guard Academy, New London, CT, USA, in 1972, the M.S. degree in optical engineering from the University of Rochester, Rochester, NY, USA, in 1977, and the Ph.D. degree in electrical engineering under the guidance of Prof. J. W. Goodman from Stanford University, Stanford, CA, USA, in 1986.

He served in the U.S. Coast Guard as an officer for ten years. After completing his Ph.D. research, he spent a year with the IBM Research Center working on optical storage problems. He became a Professor with the University of Arizona, Tucson, AZ, USA, in 1987. He is currently a Joint Professor the Department of Electronics and Communication Engineering and the College of Optical Sciences, University of Arizona. His primary research interests include holographic concepts, materials, and applications.

Dr. Kostuk is a Fellow of the Optical Society of America and the Society of Photo Instrumentation Engineers.